

## Supporting Information

### A class of novel luminescent layered double hydroxide nanotubes

Dimy Nanclares,<sup>a</sup> Alysson F. Morais,<sup>\*a</sup> Thainá Calaça,<sup>a</sup> Ivan G. N. Silva<sup>a</sup> and Danilo Mustafa<sup>a</sup>

#### S1. Materials and methods

The metal precursors used were the nitrate salts  $\text{Zn}(\text{NO}_3)_2 \cdot 6\text{H}_2\text{O}$  (98 mol%, Vetec) and  $\text{Al}(\text{NO}_3)_3 \cdot 9\text{H}_2\text{O}$  (98 mol%, Lab-Synth),  $\text{H}_3\text{BTC}$  (97 mol%, Sigma-Aldrich, powder form) and  $\text{NaOH}$  (97 mol%, Vetec, lentils) were used without further purification. The rare earth salts  $\text{Ln}(\text{NO}_3)_3 \cdot 6\text{H}_2\text{O}$  ( $\text{Ln}^{3+} = \text{La}^{3+}, \text{Pr}^{3+}, \text{Nd}^{3+}, \text{Sm}^{3+}, \text{Eu}^{3+}, \text{Gd}^{3+}, \text{Tb}^{3+}, \text{Dy}^{3+}, \text{Ho}^{3+}, \text{Er}^{3+}, \text{Tm}^{3+}, \text{Yb}^{3+}$  and  $\text{Lu}^{3+}$ ) were prepared by dissolution of  $\text{Ln}_2\text{O}_3$  (CSTARM, 99,99 mol%) in concentrated nitric acid followed by crystallization of the  $\text{Ln}(\text{NO}_3)_3 \cdot 6\text{H}_2\text{O}$  hydrated salts. The triblock copolymer Pluronic® P-123 and trimesate (benzene-1,3,5-tricarboxylate, BTC) were procured from Sigma Aldrich (São Paulo, Brazil).

##### S1.1. Synthesis of $\text{ZnAlLn}_x\text{-BTC-P123}$ LDHs

LDHs with nominal composition  $[\text{Zn}_2\text{Al}_{1-x}\text{Ln}_x(\text{OH})_6] \cdot (\text{BTC}^{3-})_{0.33}$ , named  $\text{ZnAlLn}_x\text{-BTC-P123}$ , where  $x$  denotes the substitution fraction  $x = \text{Ln}^{3+}/(\text{Ln}^{3+} + \text{Al}^{3+})$ , were synthesized by the controlled hydrolysis of  $\text{Zn}^{2+}$ ,  $\text{Al}^{3+}$  and  $\text{Ln}^{3+}$  in alkaline aqueous solution containing BTC and Pluronic® P-123 worm-like micelles. This structure-directing agent is previously prepared in 200 mL of an alkaline solution (pH 8) containing 0.15 wt% P-123 and  $11.5 \times 10^{-3} \text{ mol.L}^{-1}$  BTC. This mixture is heated to  $60^\circ\text{C}$  to promote the dissolution of P-123 and BTC and then cooled to room temperature. To optimize micellization, a second heat cycle is done. In the preparation of the LDHs, 10 mL of a  $1 \text{ mol.L}^{-1}$  solution containing  $\text{Zn}(\text{NO}_3)_2 \cdot 6\text{H}_2\text{O}$ ,  $\text{Al}(\text{NO}_3)_3 \cdot 9\text{H}_2\text{O}$  and  $\text{Ln}(\text{NO}_3)_3 \cdot 6\text{H}_2\text{O}$  in the stoichiometric ratio 2:1- $x$ : $x$  is dosed at a ratio of  $10 \text{ mL.h}^{-1}$  into the solution containing the micelles. The pH is stated at 8. After the metal solution has been consumed, the mixture is placed in oven for 48 h to optimize crystallization. Finally, the decanted solid is centrifuged and washed with deionized water till dilution of 50-100 times. To remove the polymeric structure directing agent, the resulting slurry is re-suspended twice in methanol and sonicated for 15 min. The final material is dried at  $60^\circ\text{C}$  for five days.

##### S1.2. Characterization

Thermogravimetric analysis (TGA) has been done on a TA Instruments TGA Q500 with a temperature ramp from room temperature to  $950^\circ\text{C}$  at a rate of  $5^\circ\text{C min}^{-1}$  and an air flow of  $60 \text{ mL min}^{-1}$ . Powder X-ray diffraction (PXRD) measurements were performed in a Bruker D8 Discover diffractometer in Bragg-Brentano geometry ( $\text{Cu K}\alpha$  radiation,  $\lambda = 1.5418 \text{ \AA}$ ). The data has been recorded from  $4$  to  $70^\circ 2\theta$  in steps of  $0.05^\circ$  and integration time of 1.5 s. Photoluminescence spectroscopy has been performed in an Edinburgh Instruments Spectrofluorometer FS5 equipped with a 150 W Xenon lamp as excitation source.

#### S2. Characterization

##### S2.1. Thermal properties

The thermal stability of the LDH nanotubes was characterized by thermogravimetry (Fig. S1). Five mass loss events are observed from  $30$  to  $950^\circ\text{C}$ . Below  $150^\circ\text{C}$ , a first mass loss event corresponds to the elimination of interlayer and adsorbed water. Dehydroxylation of the metal hydroxide layers occurs in the range from  $150$  to  $250^\circ\text{C}$ , as is typical for LDHs. No mass loss event indicating the presence of P-123 in the samples was observed indicating that this structure directing agent has been washed out of the samples during the extraction step.<sup>2</sup> A major mass loss event is observed from  $400$  to  $500^\circ\text{C}$ , ascribed to the decomposition of interlayer BTC.<sup>45</sup> For the samples for which formation of  $\text{Ln}(\text{BTC})$  complex was observed in PXRD, the BTC decomposition peak is composed by two subfeatures centered at different temperatures. This signalizes for the presence of at least two chemical environments for BTC in these samples, each of them related to a different phase in the solids. Indeed, specially for the samples containing  $\text{La}^{3+}$  and  $\text{Nd}^{3+}$ , for which the formation of  $\text{La}(\text{BTC})$  and  $\text{Nd}(\text{BTC})$  has been observed from PXRD, the rightmost subfeature is attributed to the decomposition of this side phases, as is the high temperature mass loss observed after  $600^\circ\text{C}$ .

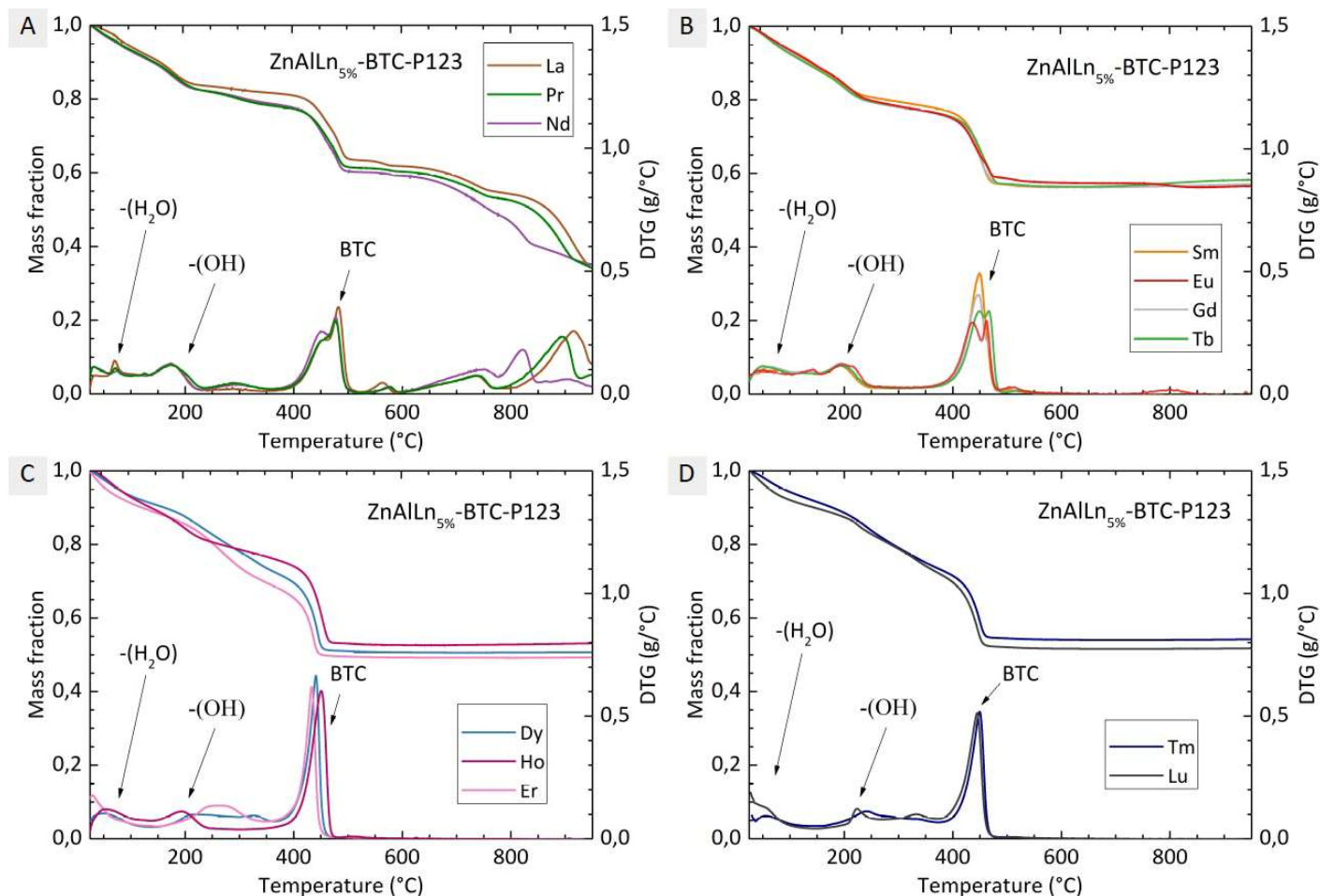


**Fig. S1** Thermogravimetric curves (TGA and DTG) for ZnAlLn<sub>5%</sub>-BTC-P123 (Ln = La, Pr, Nd, Sm, Eu, Gd, Dy, Tb, Er, Ho, Tm, Yb and Lu).

## S2.2. Structural properties

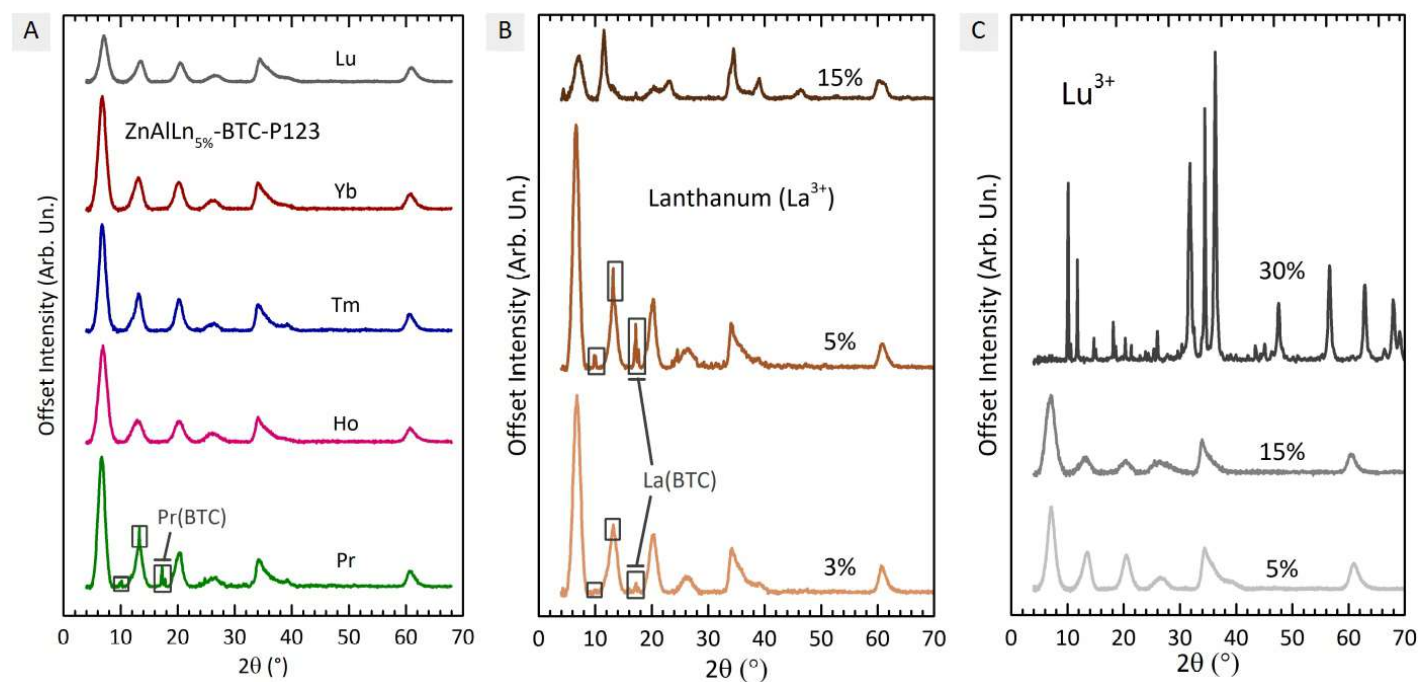


**Fig. S2** PXRD patterns for the samples  $\text{ZnAlLn}_{5\%}\text{-BTC-P123}$  for (A)  $X = 5\%$ ,  $\text{Ln} = \text{Pr, Ho, Tm, Yb}$  and  $\text{Lu}$ ; (B)  $X = 3, 5$  and  $15\%$ ,  $\text{Ln} = \text{La}$ ; and (C)  $X = 5, 15$  and  $30\%$ ,  $\text{Ln} = \text{Lu}$ .

**Table S1** Crystallographic properties of  $\text{ZnAlLn}_{5\%}\text{-BTC-P123}$

Ln	Basal spacing (nm)	FWHM (nm)	Scherrer crystallite size (nm)	Average stacking number	$d_{MM}$ (nm)
None	1.29(9)	1.21	6.6	5.1	0,303(3)
La	1.30(11)	1.51	5.3	4.1	0,304(3)
Pr	1.32(11)	1.45	5.5	4.2	0,304(3)
Nd	1.35(14)	1.75	4.6	3.4	0,3046(24)
Sm	1.35(14)	1.73	4.6	3.4	0,304(3)
Eu	1.34(11)	1.33	6.0	4.5	0,305(3)
Gd	1.32(13)	1.79	4.5	3.4	0,304(3)
Tb	1.32(13)	1.75	4.6	3.4	0,305(3)
Dy	1.30(10)	1.34	6.0	4.6	0,304(3)
Ho	1.28(12)	1.74	4.6	3.6	0,304(3)
Er	1.30(10)	1.34	6.0	4.6	0,304(3)
Tm	1.30(11)	1.43	5.6	4.3	0,305(3)
Yb	1.30(12)	1.60	5.0	3.8	0,305(3)
Lu	1.25(11)	1.58	5.1	4.1	0,304(3)

### S2.3. Morphological properties

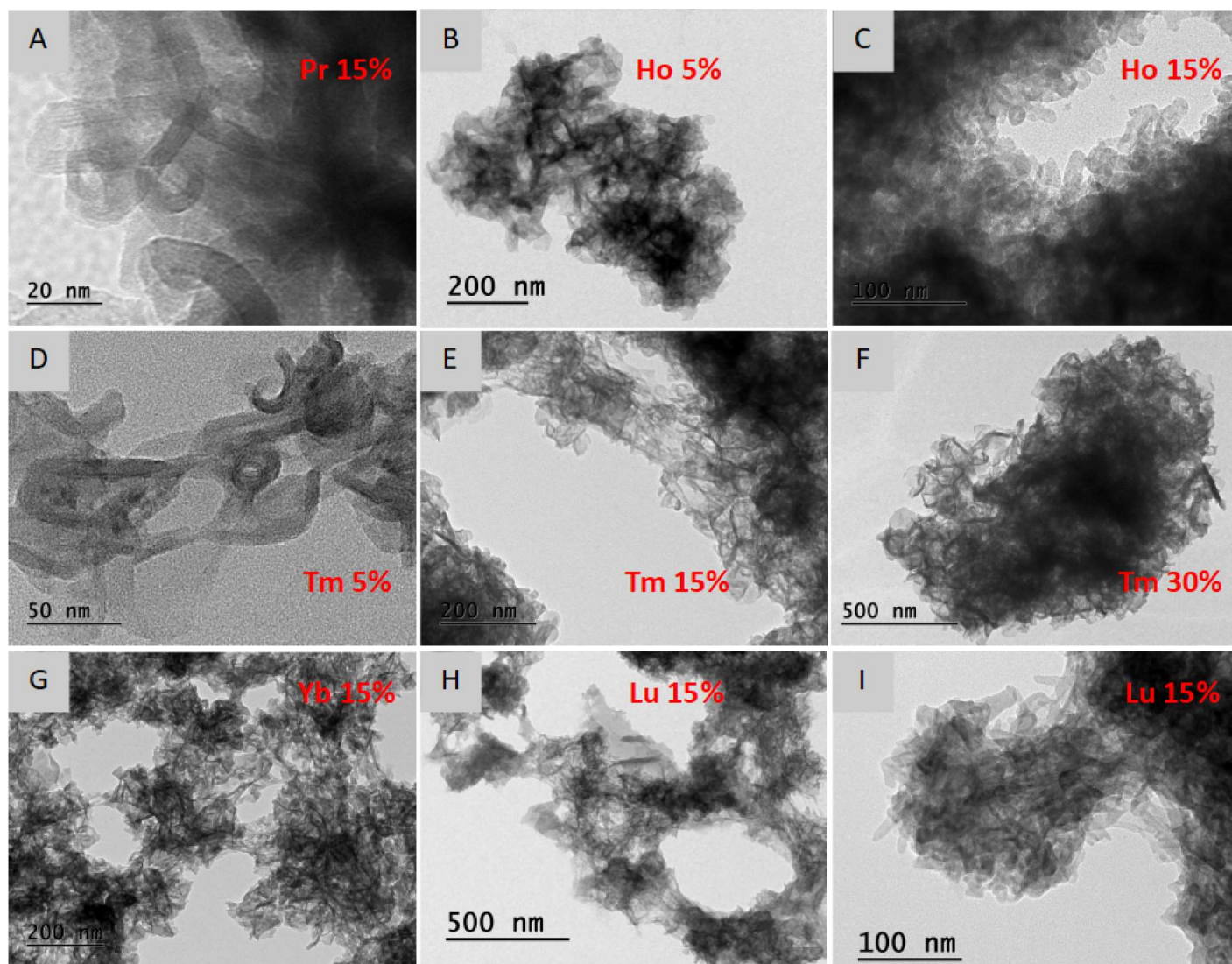


**Fig. S3** Transmission electron micrographs of ZnAlLn<sub>x%</sub>-BTC-P123: (A) Praseodymium, (B-C) Holmium, (D-F) Thulium, (G) Ytterbium and (H-I) Lutetium.



## S2.4. Photoluminescent properties

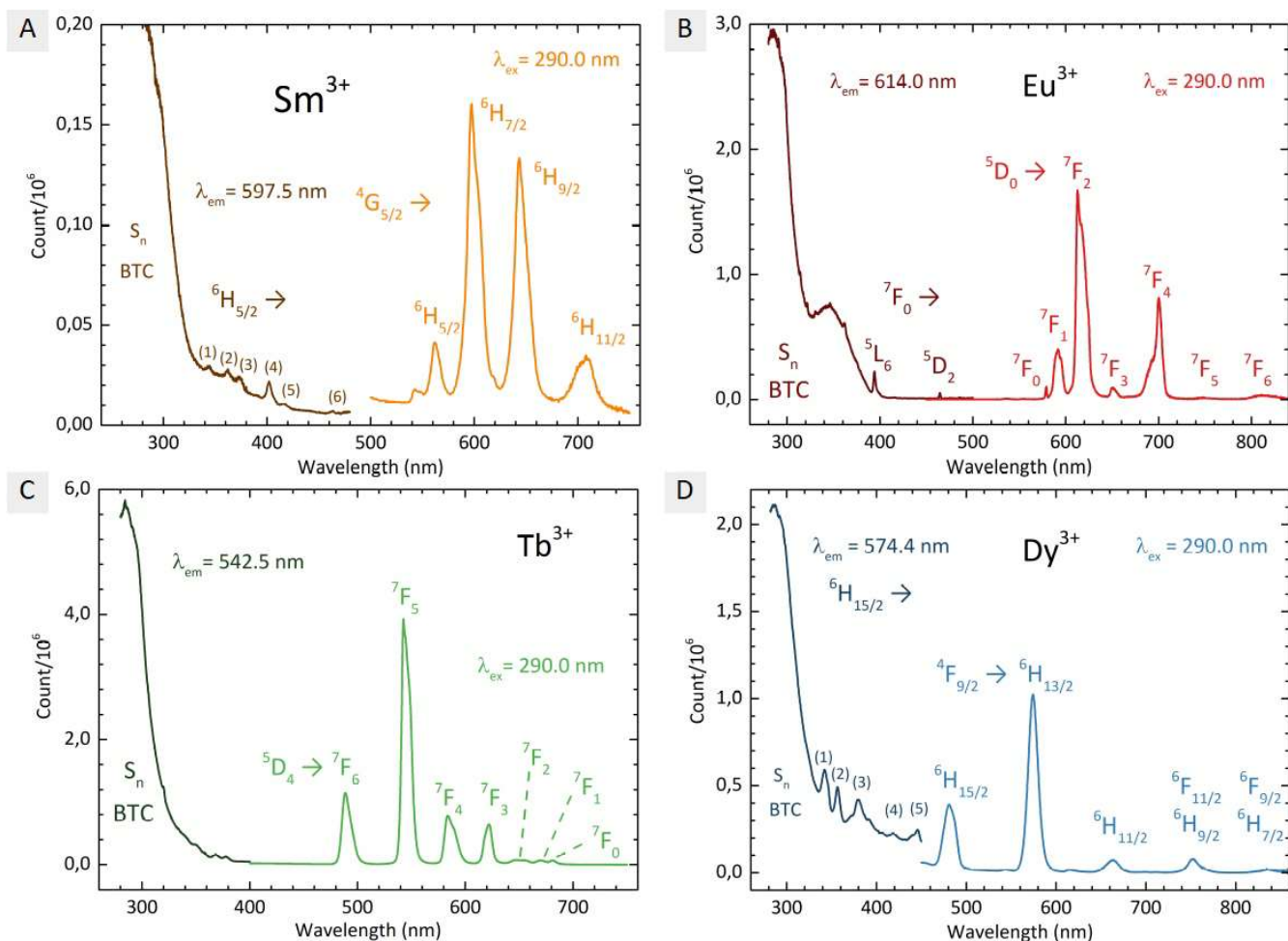


**Fig. S4** Excitation and emission spectra of ZnAlLn<sub>5</sub>%-BTC-P123 for Ln = Sm, Eu, Tb and Dy. The intraconfigurational 4f-4f transitions of the lanthanides are visible in the spectra. A - Samarium. Intraconfigurational transitions from <sup>6</sup>H<sub>5/2</sub> ground state of Sm<sup>3+</sup> are ascribed as (1) <sup>4</sup>H<sub>9/2</sub>, (2) <sup>4</sup>D<sub>3/2</sub>, (3) <sup>6</sup>P<sub>7/2</sub>, (4) <sup>6</sup>P<sub>3/2</sub>, <sup>4</sup>L<sub>13/2</sub>, (5) <sup>6</sup>P<sub>5/2</sub> and (6) <sup>4</sup>I<sub>13/2</sub>. D - Dysprosium. Intraconfigurational transitions from <sup>6</sup>H<sub>15/2</sub> ground state of Dy<sup>3+</sup> are ascribed as (1) <sup>4</sup>M<sub>15/2</sub>, <sup>6</sup>P<sub>7/2</sub>, (2) <sup>6</sup>P<sub>5/2</sub>, <sup>6</sup>P<sub>3/2</sub>, (3) <sup>4</sup>M<sub>19/2</sub>, <sup>4</sup>M<sub>21/2</sub>, <sup>4</sup>I<sub>13/2</sub>, <sup>4</sup>K<sub>17/2</sub>, <sup>4</sup>F<sub>7/2</sub>, (4) <sup>4</sup>G<sub>11/2</sub> and (5) <sup>4</sup>H<sub>15/2</sub>.

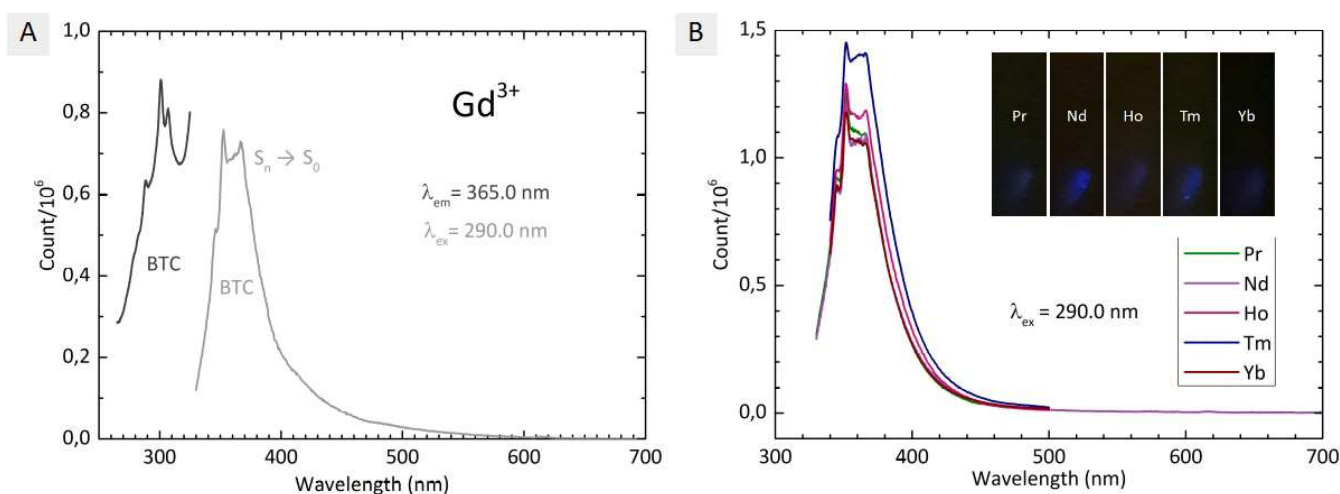


**Fig. S5** Excitation and emission spectra of ZnAlLn<sub>5%</sub>-BTC-P123 for Ln = Pr, Nd, Gd, Ho, Tm, Yb. In these materials, both fluorescence and phosphorescence of BTC were observed in the emission spectra. No emission from the lanthanide activators is observed.